

# Transition Metal Oxides as the Electrode Material for Sodium-Ion Capacitors

## Article history:

Received: 15-01-2023

Revised: 29-03-2023

Accepted: 09-04-2023

Yamini Gupta<sup>a</sup>, Poonam Siwath<sup>b</sup>, Reetika Karwasra<sup>c</sup>,  
Kriti Sharma<sup>d</sup>, S. K. Tripathi<sup>e</sup>

**Abstract:** The research of energy-storage systems has been encouraged in the last ten years by the rapid development of portable electronic gadgets. Hybrid-ion capacitors are a novel kind of capacitor-battery hybrid energy storage device that has earned a lot of interest because of their high power density while maintaining energy density and a long lifecycle. Mostly, lithium-based energy storage technology is now being studied for use in electric grid storage. But the price increment and intermittent availability of lithium reserves make lithium-based commercialization unstable. Therefore, sodium-based technologies have been proposed as potential substitutes for lithium-based technologies. Sodium-ion capacitors (SICs) are acknowledged as potential innovative energy storage technologies which have lower standard electrode potentials and lower costs than lithium-ion capacitors. However, the large radius of the sodium ion also contributes to unfavorable reaction kinetics, low energy density, and brief lifespan of SICs. Recently, transition metal oxide (TMO)-based candidates have been considered potential due to the large theoretical capacity, environmental friendliness, and low cost for SICs. This brief study summarizes current advancements in research of TMOs and sodium-based TMOs as electrode candidates for SIC applications. Also, we have covered in detail the state of the exploration and upcoming prospects of TMOs for SICs.

**Keywords:** Transition metal oxides, Electrode materials, Energy density, Power density, Sodium-ion capacitors.

<sup>a</sup> Department of Physics,  
Goswami Ganesh Dutta  
Sanatan Dharma College,  
Sector 32-C, Chandigarh,  
160030, India.

<sup>b</sup> Department of Physics, Arya  
Kanya Mahavidyalaya, Shahabad  
(M), Haryana, 136135, India.

<sup>c</sup> Department of Physics,  
Goswami Ganesh Dutta  
Sanatan Dharma College,  
Sector 32-C, Chandigarh,  
160030, India.

<sup>d</sup> Department of Physics,  
Goswami Ganesh Dutta  
Sanatan Dharma College,  
Sector 32-C, Chandigarh,  
160030, India.  
Corresponding author:  
kriti.sharma@ggdsd.ac.in

<sup>e</sup> Department of Physics, Centre  
for Advanced Study in Physics,  
Panjab University, Chandigarh,  
160014, India.  
Corresponding author:  
surya@pu.ac.in

## 1. INTRODUCTION

Scientists have made several attempts to create new and renewable energy sources, such as solar power, wind power, and wave energy driven by frequent and harmful indications of environmental deterioration, such as smog, and significantly diminished fossil fuel supplies. Yet, climate and sunlight frequently result in intermittent and fluctuating energy supply [Yang *et al.*, 2023; Halder *et al.*, 2023; Peng *et al.*, 2023; Zhang *et al.*, 2023; Thirumal *et al.*, 2023]. Therefore, the demand for electrochemical energy storage systems has grown in the market globally. Lithium-ion batteries (LIBs) and supercapacitors (SCs) have been marked significantly in the field of energy storage [Lee *et al.*, 2023; Jo *et al.*, 2023; Li *et al.*, 2023; Liu *et al.*, 2023]. LIBs have a high energy density ( $E_d$ ) of 150-250 Wh kg<sup>-1</sup>, but their power density ( $P_d$ ) is less than 1000 W kg<sup>-1</sup>, which is generally insufficient, and their cycling stability is fairly restricted (1000 cycles). This is due to the slow insertion/extraction of Li<sup>+</sup> ions in electrode materials. Because

of the quick adsorption/desorption of ions on the electrode surface, traditional electrochemical double-layer supercapacitors (EDLCs) often exhibit high  $P_d$  ( $>10,000 \text{ W kg}^{-1}$ ) and great cycling stability ( $\sim 10,000$ - $1,00,000$  cycles). Unfortunately, the  $E_d$  of EDLC (approximately  $5$ - $10 \text{ Wh kg}^{-1}$ ) is inadequate [Fan *et al.*, 2023; Sun *et al.*, 2023; Das *et al.*, 2023; Diez *et al.*, 2023; Zhang *et al.*, 2023]. Thus, the performance of ordinary LIBs and SCs has not been enough to fulfill the rising demand for high-performance energy storage devices with high  $E_d$  and  $P_d$ . To overcome this issue, researchers created a hybrid device called hybrid-ion capacitors (HICs). HICs have earned considerable interest due to the benefits of both batteries (low self-discharge and high  $E_d$ ) and SCs (stable cyclability and high  $P_d$ ) [Jia *et al.*, 2020; Deng *et al.*, 2020]. HICs comprise negative and positive electrodes that contain different charge storage mechanisms. At present, lithium-ion capacitors (LICs) are commercialized in the market for various power configurations [Zhang *et al.*, 2021]. LICs have demonstrated the integration of complementary charge storage methods of LIBs and SCs while receiving their distinct merits, drawing significant research interest. But, the key issues regarding safety and price increments due to the limited reserves are hindrances met in the growing requirements for lithium-based systems. Sodium-based energy storage devices are thought to be a viable replacement for lithium-based ones as sodium resources are relatively abundant and exhibit similar physical and chemical characteristics to lithium storage [Aristote *et al.*, 2022; Zhang *et al.*,

2020; Cai *et al.*, 2021; Zhang *et al.*, 2020]. Among all the available HICs, sodium-ion capacitors (SICs) have been chosen as potential candidates as an alternative to LICs since they can instantaneously involve high power and energy performances, involving capacitor-type cathode and battery-type anode (fig.1) candidates [Zhu *et al.*, 2020; Han *et al.*, 2021].

The study of SICs began in the year 2012 and is still in the early stages of scholarly validation with several challenges to their practical use, whereas LICs have been effectively commercialized in recent years. The commercial LICs have been provided by Taiyo Yuden and JM Energy Company [Dong *et al.*, 2021]. Nowadays, a wide range of materials has been investigated for their use as electrode materials for both LICs and SICs. Recently, transition metal oxide (TMO)-based materials are considered significant for both LICs and SICs due to their advantages over the other materials. Table 1 shows the comparison of the electrochemical performance of TMO-based electrode materials for LICs and SICs. Because of the large size of sodium ions, many battery-type electrode materials for lithium-ion storage cannot match the criteria of SIC devices. Furthermore, because the redox potential of  $\text{Na}/\text{Na}^+$  is  $0.3 \text{ V}$  greater than that of  $\text{Li}/\text{Li}^+$ , the operating voltage ranges of SICs are estimated to be slightly smaller than those of LICs, thereby influencing the energy densities of SICs. Also, the electrolyte should allow for the fast movement of  $\text{Na}^+$  ions. As a result, finding rational materials with enhanced electrochemical performance will be a future challenge for improving the overall performance of SICs.

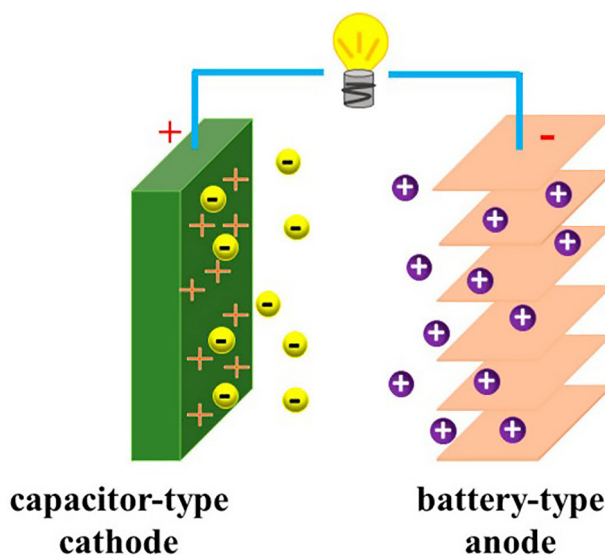


**Figure 1.** Hybrid-ion capacitor arrangement illustrated schematically. Reproduced from Han *et al.* (2021).

Device	Type	Voltage (V)	$E_d$ (Wh kg <sup>-1</sup> )	$P_d$ (W kg <sup>-1</sup> )	Capacity retention	Ref.
LiCrTiO <sub>4</sub> //AC	LIC	1-2.5	23	4000	84% after 1000 cycles	(Aravindan <i>et al.</i> , 2012)
AC/LiNi <sub>0.5</sub> C <sub>0.2</sub> Mn <sub>0.3</sub> O <sub>2</sub> //hard carbon	LIC	2.5-4.2	66.6	6500	96.45%, after 1000 cycles	(Hengheng <i>et al.</i> , 2018)
Li <sub>4</sub> Ti <sub>5</sub> O <sub>12</sub> //graphite	LIC	1.5-3.7	233	20,960	88% over 10,000	(Wang <i>et al.</i> , 2019)
LiMn <sub>2</sub> O <sub>4</sub> //AC	LIC	0-2	32.63	10,000	75.9% over 2000 cycles	(Xiang <i>et al.</i> , 2021)
TiO <sub>2</sub> /Ti <sub>3</sub> C <sub>2</sub> T <sub>x</sub> // carrot-derived porous carbon	LIC	0-4	129.4	10,000	77% after 10,000 cycles	(Zhou <i>et al.</i> , 2023)
TiO <sub>2</sub> @mesoporous carbon//AC	LIC	0-3	27.5	5000	80.5% after 10,000 cycles	(Yang <i>et al.</i> , 2017)
TiO <sub>2</sub> -coated Li <sub>4</sub> Ti <sub>5</sub> O <sub>12</sub> //AC	LIC	0.5-2.5	74.85	7500	83.3% after 5000 cycles	(Gao <i>et al.</i> , 2015)
graphene- Li <sub>4</sub> Ti <sub>5</sub> O <sub>12</sub> // graphene-sucrose	LIC	0-3	95	3000	94% after 500 cycles	(Leng <i>et al.</i> , 2013)
AC//Na <sub>0.67</sub> Mn <sub>0.75</sub> Al <sub>0.25</sub> O <sub>2</sub>	SIC	0-2.7	13	750	90% after 1000 cycles	(Tian <i>et al.</i> , 2016)
NiCo <sub>2</sub> O <sub>4</sub> //AC	SIC	0-4.5	15	300	62% after 2000 cycles	(Ding <i>et al.</i> , 2013)
TiO <sub>2</sub> @graphene//AC	SIC	1-3.8	64	1357	90% after 10,000 cycles	(Le <i>et al.</i> , 2017)
TiO <sub>2</sub> @CNT@C//bio derived AC	SIC	1-4	81.2	12,400	84% after 5000 cycles	(Zhu <i>et al.</i> , 2017)
3D-Na <sub>2</sub> Ti <sub>3</sub> O <sub>7</sub> sheets// graphene foam	SIC	1-3	55	3000	80% after 2500 cycles	(Dong <i>et al.</i> , 2016)
Na <sub>2</sub> Ti <sub>3</sub> O <sub>7</sub> @CNT//AC	SIC	0-3	59	3000	77% after 4000 cycles	(Dong <i>et al.</i> , 2015)
Nb <sub>2</sub> O <sub>5</sub> @rGO//AC	SIC	1-4.3	76	8000	66% after 3000 cycles	(Lim <i>et al.</i> , 2016)
V <sub>2</sub> O <sub>5</sub> @CNT//AC	SIC	0-2.8	38	5000	80% after 900 cycles	(Chen <i>et al.</i> , 2012)

**Table 1.** Comparison of TMO electrode materials for LICs and SICs.

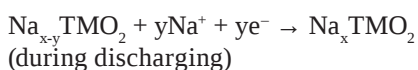
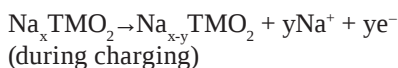
TMOs due to their large theoretical capacity are of significant concern as electrode materials for sodium storage resulting from the multiple electron transfer per metal center, and play important roles for energy-related technologies due to price advantage and ecologically benign nature [Yang *et al.*, 2018]. Some studies have also been done on TMOs as electrode materials for SICs. But there are still issues with poor conductivity, weak reversibility, significant volume changes, and sluggish redox kinetics [Wang *et al.*, 2021]. To accomplish this, binary transition metal oxides (BTMOs) and multiple anions transition metal compounds in addition to the single-ion have been created and investigated as electrode materials for SICs [Yuan

*et al.*, 2014]. Although BTMOs have substantially higher theoretical capacities and electronic conductivities than TMOs, their ability to store sodium is still constrained by the massive volume changes that occur during charge-discharge cycles and slow sodiation/desodiation reaction kinetics [Su *et al.*, 2016]. This study focuses on the review of TMOs for SICs. In this review, we conclude with an outline of recent efforts to construct high-performance SICs based on TMO electrodes. To give some inspiration for the production and design of high-performance TMOs-based electrode candidates for SICs, we conclude by sharing our thoughts on the current obstacles and potential future research areas.

## 2. BASIC PRINCIPLE AND MECHANISM OF SICs

The energy-storing process could be categorized as an electrical double layer or faraday redox reaction based on the various electrode materials. Electrolyte ions are adsorbed on the electrode-electrolyte interface to create electrical double layers in the first process. Carbon compounds with stability and a high specific area, such as carbon nanotubes (CNTs), graphene, and activated carbon (AC) are used as electrode materials. The faraday pseudocapacitance suggests that the electroactive constituent is subjected to potential deposition on the surface of the material, with fast reversible redox reactions to store the charge. A complete SIC cell has two electrodes (fig.1), with the anode made of a battery-type electrode material and the cathode typically composed of a capacitor-type electrode material separated by an electrolyte-permeable separator, all of which are submerged in the electrolyte. Sodium ions in the electrolyte intercalate and deintercalate the electrode constituent during the energy storage and conversion process. During charging, cations approach the negative electrode (battery-type), where they are stored by processes such as intercalation, conversion, and alloying, while anions are adsorbed on the positive electrode (capacitor-type). The discharge process comprises cation extraction from the negative electrode and anion desorption from the positive electrode [Zhang *et al.*, 2020; Cai *et al.*, 2021].

The general sodium storing mechanism in TMO-based materials is described through the reaction kinetics as given below [Jiang *et al.*, 2018; Karikalan *et al.*, 2017]:



## 3. ELECTRODE MATERIALS

The electrochemical characteristics of SICs are significantly influenced by the electrode materials. SICs should contain anode materials with increased surface-controlled pseudocapacitance, decreased diffusion distance, and extended lattice spacing. For instance, transition metal chalcogenides, heteroatom-doped carbon materials, transition metal oxides

and compounds, nitrides, NASICON, MXenes, and alloys are generally employed as anode materials. Regarding the cathodes, it is vital to choose materials such as porous carbon, Prussian blue, and MXenes that have strong electrical conductivity and a large specific surface area. The advancements in electrode candidates over the past few years are explained in detail in the section that follows.

### 3.1. Transition metal oxides as electrode materials for SICs

Many researchers have investigated TMOs as electrode materials for SICs. Niobium pentoxide ( $\text{Nb}_2\text{O}_5$ ), Ti-based, and other transition metals (Ni, Co, Fe, Cr, Mn, V, W, and Mo) based oxides are the several categories of electrode materials that have been investigated. The researchers employed several design and control tactics to increase the cycle life, capacity, and rate capability of the active compounds for SICs [Su *et al.*, 2016; Chen *et al.*, 2019].

Song *et al.* (2022) examined a  $\text{Mn}_3\text{O}_4@\text{TiO}_2$  nanocomposite where  $\text{Mn}_3\text{O}_4$  nanoparticles are implanted in  $\text{TiO}_2$  which serves as the anode for SICs. The nanoparticles exhibit macro- and mesopores in a hierarchically porous structure. To create a balance between the heterostructured  $\text{Mn}_3\text{O}_4/\text{TiO}_2$  surfaces and the hierarchically porous structure, the  $\text{Mn}_3\text{O}_4$  content in the nanoparticles can be changed. This balance is achieved with 30 wt%  $\text{Mn}_3\text{O}_4$  in  $\text{Mn}_3\text{O}_4@\text{TiO}_2$ , which provides a significant capacity of 247.8 mAh  $\text{g}^{-1}$  at 1 A  $\text{g}^{-1}$  current density after 1000 cycles in Sodium-ion batteries (SIBs). The fabricated SIC utilizing AC as the cathode candidate and  $\text{Mn}_3\text{O}_4@\text{TiO}_2$  as the anode candidate can attain high  $E_d$  and  $P_d$  of 106.5 Wh  $\text{kg}^{-1}$  and 10.14 kW  $\text{kg}^{-1}$ , respectively. Further, the system can deliver a superior cycle life of 92.8% after 5000 cycles. Wang *et al.* (2022) synthesized single-crystal transition metal selenite  $\text{CoSeO}_3$  nanocomposites with a particle size spanning from 80 to 200 nm for SICs. In  $\text{CoSeO}_3\|\text{Na}$  SIBs, a specific capacity of 280 mAh  $\text{g}^{-1}$  is attained at 0.01 mA  $\text{g}^{-1}$  current density. Additionally, the associated  $\text{CoSeO}_3\|\text{AC}$  SICs have a  $P_d$  of 2000 W  $\text{kg}^{-1}$  along with an enhanced  $E_d$  of 51 Wh  $\text{kg}^{-1}$  and a capacity retention of 72% after 3000 cycles at 1 A  $\text{g}^{-1}$ .

Liang *et al.* (2022) prepared layered  $\text{Fe}_2(\text{MoO}_4)_3$  (L-FMO) material using the solvothermal method and utilized it as an anode candidate for SICs. The enhanced extrinsic pseudocapacitance helps the L-FMO material to have quick kinetics, a large



capacity for storing sodium, and a long lifetime. A  $P_d$  of 20,050 W kg<sup>-1</sup> and a high  $E_d$  of 227.2 Wh kg<sup>-1</sup> are achieved using the L-FMO material in SICs. They also exhibit better cyclic stability, with a poor capacity degradation over 3000 cycles at 1 A g<sup>-1</sup>. Fig. 2 depicts the X-ray diffraction (XRD) pattern of L-FMO and the high-resolution X-ray photoelectron spectroscopy (XPS) spectrum of Fe 2p, Mo 3d, and O 1s. Furthermore, field emission transmission electron microscopy (FESEM), transmission electron microscopy (TEM), fast Fourier transform (FFT) pattern, high-resolution transmission electron microscopy (HRTEM), and Energy-dispersive

X-ray spectroscopy (EDS) mapping images of L-FMO have also been shown in fig.2. Zhu *et al.* (2017) reported SIC that uses TiO<sub>2</sub>@CNT@C composite as an anode candidate and biomass-derived carbon material as a cathode candidate with high surface area in an organic electrolyte. The sophisticated design of the electrospun TiO<sub>2</sub>@CNT@C nanorods exhibits great cycle stability and rate capability in the half configuration of cells. The assembled SIC offers a high  $P_d$  of 12,400 W kg<sup>-1</sup> and high  $E_d$  of 81.2 Wh kg<sup>-1</sup> within 1-4 V. The SIC retains 85.3% of its capacity after 5000 cycles of testing at 1 A g<sup>-1</sup>.

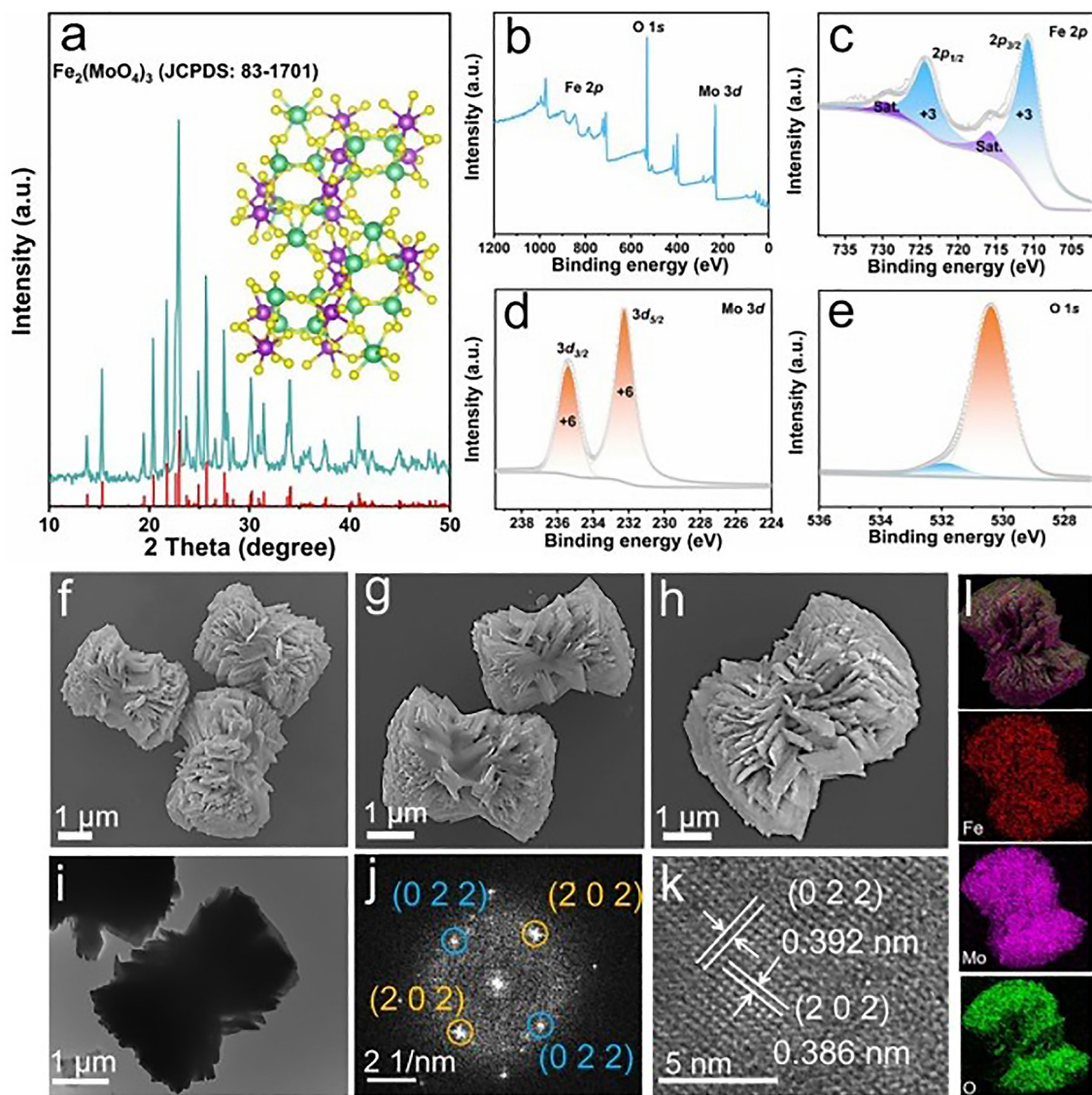


**Figure 2.** (a) XRD-plot of L-FMO and matching crystal structure, (b) XPS spectrum of (c) Fe 2p, (d) Mo 3d, and (e) O 1s, (f-h) FESEM, (i) TEM, (j) FFT plot, (k) HRTEM, (l) and EDS mapping pictures of L-FMO. Reproduced from Liang *et al.* (2022).

Zhang *et al.* (2018) prepared a layered  $\text{MnO}_2/\text{CNT}$  composite, a typical pseudocapacitive material for SICs. An outstanding capacity retention of about 90% over 5000 cycles and a high specific capacitance of  $322.5 \text{ F g}^{-1}$  at  $0.5 \text{ A g}^{-1}$  are both provided by the composite. The layered  $\text{MnO}_2/\text{CNTs}$  as a cathode candidate, polyimide organic as an anode candidate, and Na-ion water-in-salt electrolyte work together to create a synergistic effect that allows the as-assembled SIC to achieve the capacity retention of 77 % after 10,000 cycles along with high  $E_d$  and  $P_d$  of  $78.5 \text{ Wh kg}^{-1}$  and  $11,000 \text{ W kg}^{-1}$ . Liu *et al.* (2020) reported sodium-ion conducting gel polymer serving as the electrolyte and layered  $\text{FeTiO}_3$  nanocomposite as the anode to build a quasi-solid-state SIC. The end product, which is among the most advanced SIC has a high  $P_d$  of  $6750 \text{ W kg}^{-1}$  and a high  $E_d$  of  $79.8 \text{ Wh kg}^{-1}$ . Additionally, the built SIC demonstrates a capacity retention of 80% with a super cycling stability of 2000 cycles.

Yang *et al.* (2018) researched  $\text{NiCo}_2\text{O}_4$  particles inside a nitrogen-doped graphene framework for SICs. Good electronic conductivity is ensured

by the graphene structure, which also acts as a buffer to lessen  $\text{NiCo}_2\text{O}_4$  size variations. The composite electrode in a half configuration of the cell can show a capacity of around  $450 \text{ mAh g}^{-1}$  at  $1/10 \text{ A g}^{-1}$  after the hundredth cycle. AC serving as the cathode candidate and the composite serving as the anode candidate, a full-cell SIC produced an  $E_d$  and  $P_d$  of  $48.8 \text{ Wh kg}^{-1}$  and  $9750 \text{ W kg}^{-1}$  with better cycle stability. Gao *et al.* (2021) synthesized bimetallic  $\text{MnMoO}_4$  which performs satisfactorily in lithium storage. A SIC based on  $\text{Na}_3\text{V}_2(\text{PO}_4)_3$  as a cathode candidate and  $\text{MnMoO}_4$  as an anode candidate is assembled which exhibits  $P_d$  of 4000 and  $240 \text{ W kg}^{-1}$  and high  $E_d$  of 88 and  $168 \text{ Wh kg}^{-1}$ . This is due to the pseudocapacitive nature of the  $\text{MnMoO}_4$  candidate in sodium storage. Fig. 3 depicts the diagram of the full cell configuration of SIC consisting of  $\text{MnMoO}_4@\text{C}/\text{Na}_3\text{V}_2(\text{PO}_4)_3$  with three galvanostatic charge-discharge (GCD) curves at  $1/10 \text{ A g}^{-1}$ , rate performance, GCD curves at different current densities, and cyclic performance of the full cell configuration. Ragone scheme distinguishing the equipped SIC with other defined SIBs and SICs has also been shown in fig. 3.

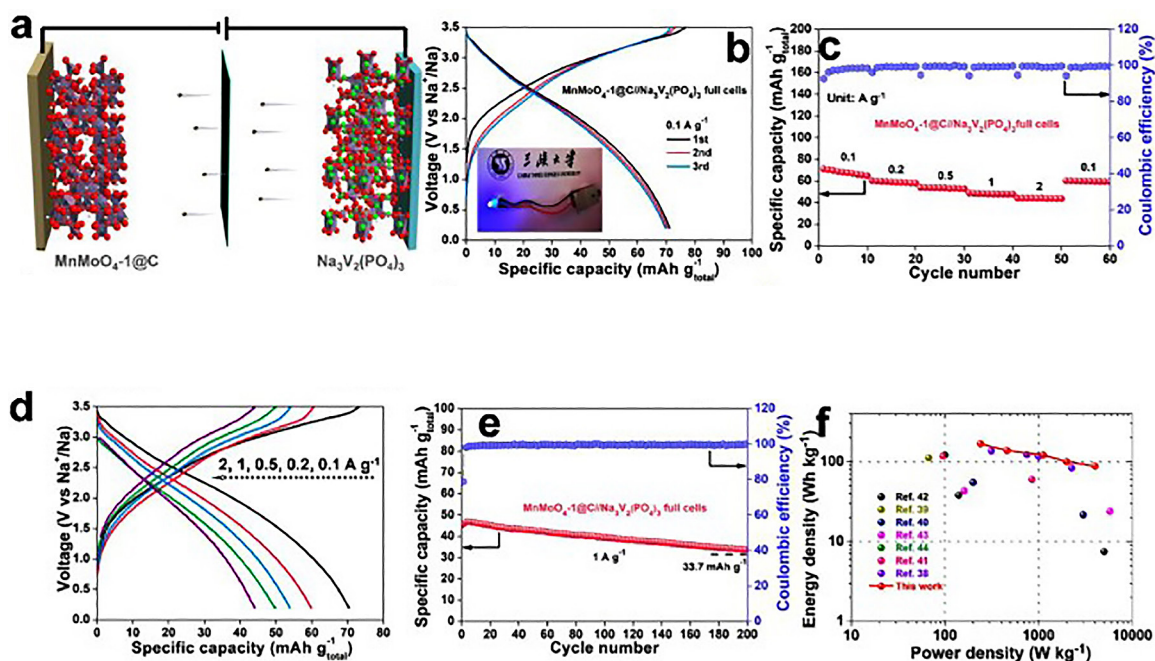


**Figure 3.** (a) Diagram of the full configuration. (b) SIC consisting of  $\text{MnMoO}_4@\text{C}/\text{Na}_3\text{V}_2(\text{PO}_4)_3$  with three GCD curves at  $1/10 \text{ A g}^{-1}$ . (c) Rate performance, (d) GCD curves at various current densities, and (e) Cyclic stability of the full cell comprising of  $\text{MnMoO}_4@\text{C}/\text{Na}_3\text{V}_2(\text{PO}_4)_3$ . (f) Ragone scheme distinguishing the equipped SIC from other defined SIBs and SICs.

Reproduced from Gao *et al.* (2021).

Qin *et al.* (2020) reported Mn<sup>2+</sup>/Nb<sup>5+</sup> embedded in linked hollow carbon nano boxes (NaNbO<sub>3</sub>@HCNb and MnO@HCNb) using a chemical vapor deposition technique. As a result, the MnO@HCNb electrode exhibits a good lifecycle of greater than 10,000 cycles with capacity retention of 88.6% and exceptional rate performance, which is uncommon for oxide-based anodes. These hybrid ion storage systems demonstrate consistent capacitive electrochemical activity and favorable compatibility. A complete SIC cell using AC as a cathode exhibits a high E<sub>d</sub> of 56.4 Wh kg<sup>-1</sup> at 1.8 Wh kg<sup>-1</sup> and 116 Wh kg<sup>-1</sup> at 99 Wh kg<sup>-1</sup>. Fang *et al.* (2020) prepared a self-supporting foam electrode as TiO<sub>2</sub>@reduced graphene oxide (M-TiO<sub>2</sub>@rGO) for SICs. Excellent rate ability, better capacity, and enhanced cycle performance are the results of the

pseudocapacitance-dominated process. SICs made of M-TiO<sub>2</sub>@rGO/ hierarchical porous AC and sodium complete cells made of M-TiO<sub>2</sub>@rGO/Na<sub>3</sub>V<sub>2</sub>(-PO<sub>4</sub>)<sub>3</sub> are constructed. The capacity of as prepared SIB is 177.1 mAh g<sup>-1</sup> at 0.5 A g<sup>-1</sup>, and its capacity retention after 200 cycles is 74%. Maximum E<sub>d</sub> and P<sub>d</sub> for the SIC are 101.2 Wh kg<sup>-1</sup> and 10,103.7 W kg<sup>-1</sup>, respectively. After 10,000 cycles, it exhibits an energy retention of 84.7% at 1.0 A g<sup>-1</sup>.

In brief, we have summarized TMOs as electrode materials for SICs with enhanced performance. An outline of TMO as electrode materials for SICs has been shown in table 2. Further, research is still being carried out on sodium-based TMOs as electrode constituents for SICs due to the abundance of Na and price advantages of sodium resources which makes it facile for production at a commercial scale.

Material	Specific capacitance / Material	Electrolyte	E <sub>d</sub> (Wh kg <sup>-1</sup> )	P <sub>d</sub> (W kg <sup>-1</sup> )	Capacity retention	Ref.
Mn <sub>3</sub> O <sub>4</sub> @TiO <sub>2</sub> //AC	247.8 mAh g <sup>-1</sup> / Mn <sub>3</sub> O <sub>4</sub> @TiO <sub>2</sub>	1 M NaPF <sub>6</sub> in DME	106.5	10,140.5	92.8% after 5000 cycles.	(Song <i>et al.</i> , 2022)
CoSeO <sub>3</sub> //AC	280 mAh g <sup>-1</sup> / CoSeO <sub>3</sub>	1 M NaClO <sub>4</sub> in PC: DMC with FEC	51	2000	72% after 3000 cycles.	(Wang <i>et al.</i> , 2022)
Fe <sub>2</sub> (MoO <sub>4</sub> ) <sub>3</sub> //AC	130.3 mAh g <sup>-1</sup> / Fe <sub>2</sub> (MoO <sub>4</sub> ) <sub>3</sub>	1 M NaClO <sub>4</sub> in EC: DEC.	227.2	20,050	88.1% after 1000 cycles	(Liang <i>et al.</i> , 2022)
TiO <sub>2</sub> @CNT@C//biomass derived AC	165 mAh g <sup>-1</sup> / TiO <sub>2</sub> @CNT@C	1 M NaClO <sub>4</sub> in EC: PC	81.2	12,400	85.3% after 5000 cycles	(Zhu <i>et al.</i> , 2017)
MnO <sub>2</sub> /CNT//polyimide	322.5 F g <sup>-1</sup> / MnO <sub>2</sub> /CNT	17 mol NaClO <sub>4</sub> /1 L H <sub>2</sub> O	78.5	11,000	77% after 10000 cycles	(Zhang <i>et al.</i> , 2018)
FeTiO <sub>3</sub> //AC	334.2 mAh g <sup>-1</sup> / FeTiO <sub>3</sub>	1 M NaClO <sub>4</sub> in EC: DEC	79.8	6750	80% after 2000 cycles	(Liu <i>et al.</i> , 2020)
NiCo <sub>2</sub> O <sub>4</sub> //AC	450 mAh g <sup>-1</sup> / NiCo <sub>2</sub> O <sub>4</sub>	1 M NaPF <sub>6</sub> in DEG: DME	48.8	9750	83.7% after 4000 cycles	(Yang <i>et al.</i> , 2018)
MnMoO <sub>4</sub> //Na <sub>3</sub> V <sub>2</sub> (PO <sub>4</sub> ) <sub>3</sub>	298.7mAh g <sup>-1</sup> / MnMoO <sub>4</sub>	1 M NaPF <sub>6</sub> in EC: DMC	168	4000	—	(Gao <i>et al.</i> , 2021)
MnO@HCNb//AC	91.7 mAh g <sup>-1</sup> / MnO@HCNb	1 M NaClO <sub>4</sub> in EC: DEC	56.4	1800	88.6% after 10,000 cycles	(Qin <i>et al.</i> , 2020)
TiO <sub>2</sub> @rGO//hierarchical porous AC	308 mAh g <sup>-1</sup> / TiO <sub>2</sub> @rGO	1 M NaClO <sub>4</sub> in EC: DMC: EMC	101.2	10,103.7	84.7% after 10,000 cycles	(Fang <i>et al.</i> , 2020)

Dimethyl ether: DME, Propylene carbonate: PC, Diethyl carbonate DEC, Fluoroethylene carbonate: FEC, Ethylene carbonate: EC, Dimethyl carbonate: DMC, Diethylene glycol: DEG, Ethyl methyl carbonate: EMC

**Table 2.** Outline of TMO as electrode materials for SICs.



### 3.2. Sodium-based transition metal oxide electrode materials for SICs

Some researchers have investigated sodium-based TMOs as electrode materials for SICs to obtain high-performance grid-scale energy storage devices. Sodium-based electrode materials are preferred over others due to the abundance and price advantage of sodium resources in the earth's crust.

Maurya *et al.* (2021) prepared a 3D-nanofibrous  $\text{Na}_2\text{Zn}_2\text{TeO}_6$  (NZTO)-implanted poly (vinylidene fluoride-co-hexafluoropropylene) (PVDF-HFP) electrolyte. AC is employed as the cathode and  $\text{Na}_{0.67}\text{Co}_{0.7}\text{Al}_{0.3}\text{O}_2$  (battery-type) as an anode to create a coin cell-style SIC. The manufactured SIC,  $\text{Na}_{0.67}\text{Co}_{0.7}\text{Al}_{0.3}\text{O}_2/\text{AC}$ , can produce a capacity retention of 84% up to 1000 cycles with a specific capacity of  $99.375 \text{ F g}^{-1}$  at  $1 \text{ A g}^{-1}$ . A  $P_d$  of  $1.6 \text{ kW kg}^{-1}$  and  $E_d$  of  $35.33 \text{ Wh kg}^{-1}$  were displayed by the SIC, respectively. Que *et al.* (2017) reported  $\text{Na}_2\text{Ti}_2\text{O}_{5-x}$  nanowire arrays as SIC anode to improve the  $\text{Na}^+$  reaction kinetics. A SIC device is fabricated with an rGO/AC film cathode and  $\text{Na}_2\text{Ti}_2\text{O}_{5-x}$  anode which can deliver  $P_d$  of  $240 \text{ W kg}^{-1}$  and high-level  $E_d$  of  $70 \text{ Wh kg}^{-1}$ . Volumetric  $E_d$  of  $15.6 \text{ Wh L}^{-1}$  depending on the entire volume and a

high  $P_d$  of  $120 \text{ W L}^{-1}$  was obtained with outstanding cyclic stability of 82.5% over 5000 cycles.

Gu *et al.* (2019) selected zeolitic imidazolate framework-8 (ZIF-8) derived carbon (ZDC) as an anode candidate and battery-type P2- $\text{Na}_{0.67}\text{Co}_{0.5}\text{Mn}_{0.5}\text{O}_2$  (P2-NCM) as a cathode candidate for the fabrication of SICs. The ZDC/P2-NCM SIC demonstrated a high  $P_d$  ( $12.75 \text{ kW kg}^{-1}$ ) and an  $E_d$  ( $18.8 \text{ Wh kg}^{-1}$ ) due to the high-rate performance and kinetic match of both electrodes. Fig. 4 depicts the diagram of ZDC//P2-NCM coin-type SIC along with the electrochemical performance of the full-cell SIC, GCD, Cyclic Voltammetry (CV) curves at  $2\text{--}10 \text{ mV s}^{-1}$  scan rates, and cycling stability with coulombic efficiency at a current density of  $5 \text{ A g}^{-1}$ . Chen *et al.* (2018) described a unique  $\text{Na}_{0.44}\text{MnO}_2$  nanorod-based symmetric SIC.  $\text{Na}_{0.44}\text{MnO}_2$  offers shorter diffusion channel lengths with its distinctive iso-oriented properties and nanoarchitecture for both electrical and sodium-ion transport and lowers the stress related to the insertion and extraction of  $\text{Na}^+$ . The symmetric device makes use of these advantages to retain a capacitance of 85.2% after 5000 cycles and attain an enhanced  $P_d$  of  $2.4327 \text{ kW kg}^{-1}$  with an  $E_d$  of  $27.9 \text{ Wh kg}^{-1}$ .

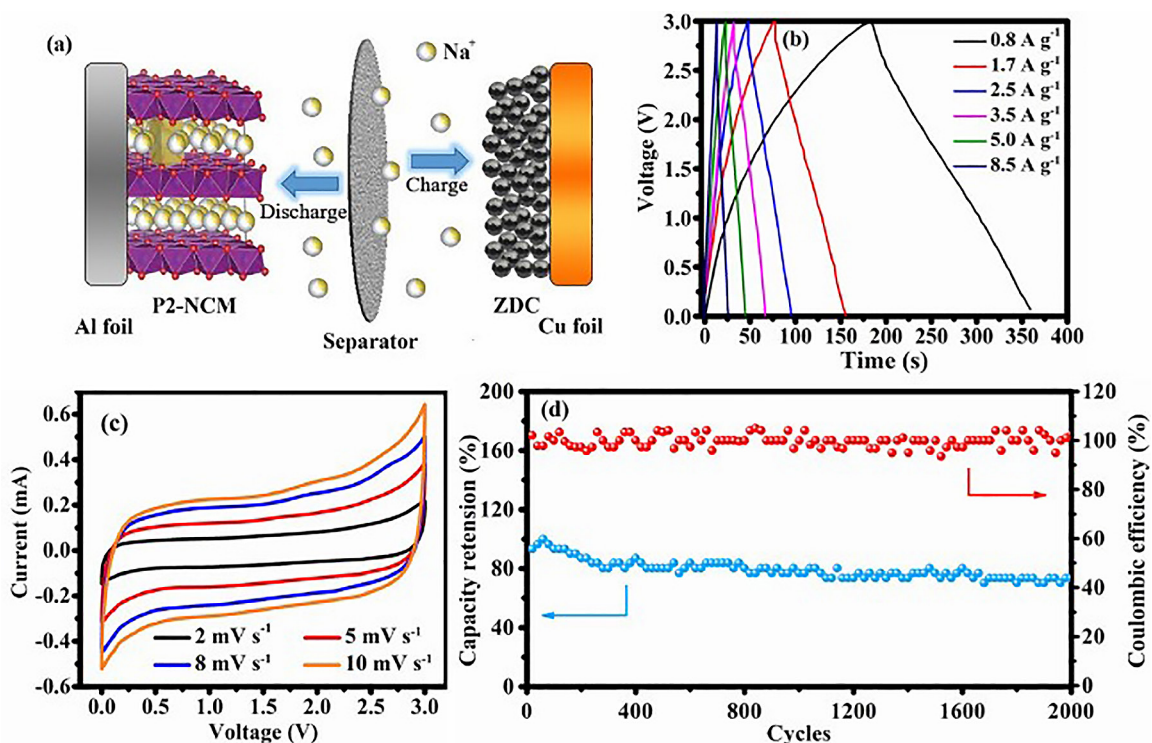


**Figure 4.** (a) Diagrammatical representation of ZDC//P2-NCM based SIC, (b-d) Electrochemical activity of the ZDC//P2-NCM based SIC, (b) GCD, (c) CV curves at different scan rates of 2, 5, 8 and  $10 \text{ mV s}^{-1}$ , (d) Cycling stability with Coulombic efficiency at  $5 \text{ A g}^{-1}$ . Reproduced from Gu *et al.* (2019).



Gao *et al.* (2018) used  $\text{Na}_2\text{Ti}_3\text{O}_7$  arrays with porous structure acting as the anode and CNTs on Al foils acting as the cathode to assemble SIC. The designed SICs can provide a  $P_d$  of  $825 \text{ W kg}^{-1}$  and a high  $E_d$  of  $49 \text{ Wh kg}^{-1}$  in the voltage range of 1-4 V. The SICs displayed the  $P_d$  of  $4000 \text{ W kg}^{-1}$  at an  $E_d$  of  $35.6 \text{ Wh kg}^{-1}$ . The SICs, on the other hand, had improved electrochemical performance at  $3.3 \text{ A g}^{-1}$ , with a 73.89% capacity retention after 2000 cycles. Bhat *et al.* (2018) examined the structural features of hydrothermally produced nanostructured  $\text{Na}_2\text{Ti}_9\text{O}_{19}$  as it undergoes electrochemical cycling. Additionally,  $\text{Na}_2\text{Ti}_9\text{O}_{19}$  exhibits superior  $\text{Na}^+$  kinetics with a capacitive behavior of 86% at  $1.0 \text{ mV s}^{-1}$ , representing that it would prove to be a beneficial anode candidate for a hybrid device that stores sodium ions. Utilizing  $\text{Na}_2\text{Ti}_9\text{O}_{19}$  as the anode candidate and AC as the cathode candidate, a complete cell hybrid SIC with an  $E_d$  and  $P_d$  of  $54 \text{ Wh kg}^{-1}$  and  $5000 \text{ W kg}^{-1}$  is created.

Dong *et al.* (2015) prepared  $\text{Na}_2\text{Ti}_3\text{O}_7$ @CNTs as an anode candidate for SICs. The  $\text{Na}_2\text{Ti}_3\text{O}_7$ @CNT composite demonstrates remarkable electrochemical activity with superb cyclic stability and rate capability due to the distinctive 1-dimensional

nanoarchitecture and the occurrence of a pseudocapacitive charge-storing nature. A SIC is also created employing  $\text{Na}_2\text{Ti}_3\text{O}_7$ @CNT as an anode candidate and AC acting as a cathode candidate (made from the outer shell of peanuts). This SIC offers high  $P_d$  and  $E_d$  of  $3000 \text{ W kg}^{-1}$  and  $58.50 \text{ Wh kg}^{-1}$  with a superior life cycle. Fig. 5 shows the diagrammatical representation of SICs, GCD curves, and cycling stability experienced for 4000 cycles at  $4/10 \text{ A g}^{-1}$ . Ragone outline of the hybrid gadgets compared to the numerous described LICs and SICs has also been depicted in fig.5. Kim *et al.* (2020) described a layered tunnel,  $\text{Na}_{0.5}\text{Mn}_{0.5}\text{Co}_{0.48}\text{Mg}_{0.02}\text{O}_2$  composite as an electrode material for SICs, whose binary structure was validated by scanning electron microscope and high-resolution transmission electron microscope. Along with the occurrence of  $\text{Mg}^{2+}$  ions as well as the 3D tunnel and 2D layered structure, a high capacity of  $145 \text{ mAh g}^{-1}$  at  $0.085 \text{ A g}^{-1}$  with a better rate capability and cyclic stability is also produced. A battery-type electrode made of a layered-tunnel structured composite and a counter electrode made of commercial AC is used to create a SIC. A  $35 \text{ Wh kg}^{-1}$  maximum  $E_d$  and better cyclic stability were displayed by the SIC, which retained 72% of  $E_d$  after 3000 cycles.

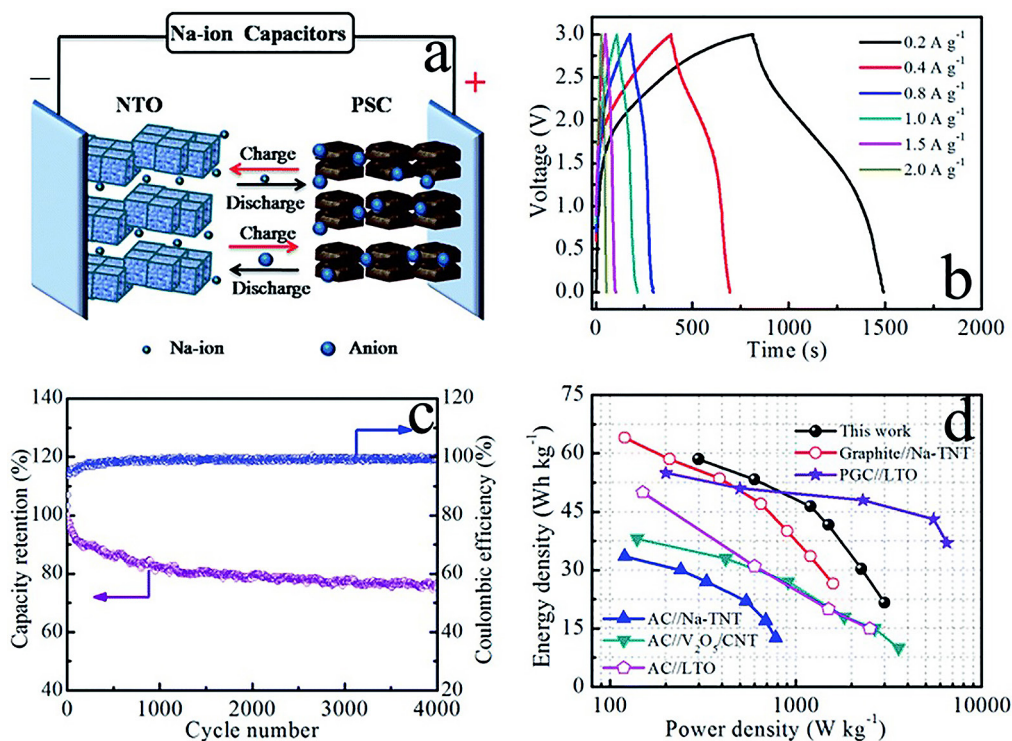


**Figure 5.** (a) Diagram of SICs comprising of anode and cathode, (b) GCD curves, (c) Cycling stability performance done for 4000 cycles at  $4/10 \text{ A g}^{-1}$ . (d) Ragone outline of the hybrid gadgets compared to the numerous stated LICs and SICs. Reproduced from Dong *et al.* (2015).

Liu *et al.* (2020) reported Na<sub>2</sub>Ti<sub>7</sub>O<sub>15</sub>/graphene as an anode candidate using an atomic layer deposition (ALD) approach, resulting in Na<sub>2</sub>Ti<sub>7</sub>O<sub>15</sub> with an interwoven structure and graphene nanosheets with an extremely high aspect ratio. The composite offers 90% cyclic stability retention at 8.85 A g<sup>-1</sup> after 10,000 cycles with a capacity of 60 mAh g<sup>-1</sup> at 17.7 A g<sup>-1</sup>. The assembled SIC can distribute high P<sub>d</sub> and E<sub>d</sub> of 25,000 W kg<sup>-1</sup> and 16 Wh kg<sup>-1</sup>. Gui *et al.* (2019) researched Na<sub>2</sub>Ti<sub>2</sub>O<sub>5</sub> nanosheet array anode which exhibits 66% capacity retention at 120 C, superior Initial Coulombic Efficiency of 91%, and high cycle Coulombic Efficiency of 100%. A SIC gadget is invented using a commercially available AC as a cathode candidate and a Na<sub>2</sub>Ti<sub>2</sub>O<sub>5</sub> array as an anode candidate. This device exhibits long

cyclic stability of more than 10,000 cycles and high E<sub>d</sub> of 0.0172 Wh cm<sup>-3</sup> and 54.50 Wh kg<sup>-1</sup>.

As summarized above, SICs have demonstrated encouraging P<sub>d</sub>/E<sub>d</sub>. An outline of sodium-based TMO as electrode materials for SICs has been shown in table 3. It should be emphasized that the kinetic behavior and decay process of electrode materials require more in-depth research for SICs. Therefore, exploring battery-type candidates with intercalated/surface pseudocapacitive nature through structural strategy and management, surface/interface, and particular nanostructures, requires a lot of work. Additionally, creating compounds with improved conductivity is required for the enlargement of high-staging electrodes for SIC commercialization.

Material	Specific capacitance/ Material	Electrolyte	E <sub>d</sub> (Wh kg <sup>-1</sup> )	P <sub>d</sub> (W kg <sup>-1</sup> )	Capacity retention	Ref.
Na <sub>0.67</sub> Co <sub>0.7</sub> Al <sub>0.3</sub> O <sub>2</sub> //AC	99.375 F g <sup>-1</sup> / Na <sub>0.67</sub> Co <sub>0.7</sub> Al <sub>0.3</sub> O <sub>2</sub>	1M NaPF <sub>6</sub> in EC: DMC	35.33	1600	84% after 1000 cycles	(Maurya <i>et al.</i> , 2021)
Na <sub>2</sub> Ti <sub>2</sub> O <sub>5-x</sub> //rGO/AC	225 mAh g <sup>-1</sup> / Na <sub>2</sub> Ti <sub>2</sub> O <sub>5-x</sub>	1 mol L <sup>-1</sup> NaClO <sub>4</sub> in EC: DMC	70	240	82.5% after 5000 cycles.	(Que <i>et al.</i> , 2017)
ZDC// P2-Na <sub>0.67</sub> Co <sub>0.5</sub> Mn <sub>0.5</sub> O <sub>2</sub>	170 mAh g <sup>-1</sup> / Na <sub>0.67</sub> Co <sub>0.5</sub> Mn <sub>0.5</sub> O <sub>2</sub>	1 mol L <sup>-1</sup> NaClO <sub>4</sub> in EC: PC	18.8	12,750	—	(Gu <i>et al.</i> , 2019)
Na <sub>0.44</sub> MnO <sub>2</sub> // Na <sub>0.44</sub> MnO <sub>2</sub>	115.3 mAh g <sup>-1</sup> / Na <sub>0.44</sub> MnO <sub>2</sub>	1 mol L <sup>-1</sup> NaClO <sub>4</sub> in EC: DMC	27.9	2432.7	85.2% after 5000 cycles	(Chen <i>et al.</i> , 2018)
Na <sub>2</sub> Ti <sub>3</sub> O <sub>7</sub> //CNT	105.5 mAh g <sup>-1</sup> / Na <sub>2</sub> Ti <sub>3</sub> O <sub>7</sub>	1 M NaClO <sub>4</sub> in EC: DEC	35.6	4000	73.89% after 2000 cycles	(Gao <i>et al.</i> , 2018)
Na <sub>2</sub> Ti <sub>9</sub> O <sub>19</sub> //AC	220 mAh g <sup>-1</sup> / Na <sub>2</sub> Ti <sub>9</sub> O <sub>19</sub>	1 M NaPF <sub>6</sub> in EC: DMC	54	5000	75% after 2000 cycles	(Bhat <i>et al.</i> , 2018)
Na <sub>2</sub> Ti <sub>3</sub> O <sub>7</sub> @CNTs//AC	292 mAh g <sup>-1</sup> / Na <sub>2</sub> Ti <sub>3</sub> O <sub>7</sub> @CNTs	1 M NaClO <sub>4</sub> in EC: PC with FEC	58.5	3000	75% after 4000 cycles	(Dong <i>et al.</i> , 2015)
Na <sub>0.5</sub> Mn <sub>0.5</sub> Co <sub>0.48</sub> Mg <sub>0.02</sub> O <sub>2</sub> //AC	145 mAh g <sup>-1</sup> / Na <sub>0.5</sub> Mn <sub>0.5</sub> Co <sub>0.48</sub> Mg <sub>0.02</sub> O <sub>2</sub>	1 M NaClO <sub>4</sub> in PC with FEC	35	150	72% after 3000 cycles	(Kim <i>et al.</i> , 2020)
Na <sub>2</sub> Ti <sub>7</sub> O <sub>15</sub> /graphene// AC	60 mAh g <sup>-1</sup> / Na <sub>2</sub> Ti <sub>7</sub> O <sub>15</sub> / graphene	1 M NaClO <sub>4</sub> in EC: DEC with FEC	16	25,000	90% after 10,000 cycles	(Liu <i>et al.</i> , 2020)

**Table 3.** Outline of Sodium-based TMO electrode materials for SICs.

#### 4. CHALLENGES AND FUTURE PERSPECTIVES

The SICs are predicted to play key roles in energy storage industries due to their high  $E_d$ , high  $P_d$ , and earth-abundant sodium supplies. Yet, SICs are still in their infancy, and further study and investigation are required. The battery-type electrode, capacitive-type electrode, and electrolyte engineering all have a substantial influence on the energy-power characteristics and cycle stability of SICs. Finding sodium-ion electrode materials with quick electrochemical kinetics and high capacity is critical for the development of improved SICs. Because of the large theoretical capacity, low price, and environment-friendly nature of TMO-based materials, SICs using TMO-based materials as an electrode are particularly sustainable prospects. Several tactics, including morphological design, porous structure modification, and heteroatom doping, can be used to improve the redox kinetics of battery-type electrodes and the capacitance of capacitive electrodes, allowing for high  $E_d$  and high  $P_d$ . Following that, in addition, to increasing the electrochemical performance of electrode materials, the rational design of electrode structures is critical. 3D architectural electrodes can offer channels for electrical conduction and ion migration, as well as voids that reduce electrode strain during the charging/discharging process. Moreover, employing 3D architectural electrodes can result in SIC devices that do not require an extra current collector or binder, as well as lowering the difficulty of designing flexible devices for wearable electronics. Last but not least, the electrolytes must still be tuned to assure the safety and performance of SICs. Aqueous energy storage technologies, in particular, provide significant benefits in terms of cost, high safety, and large power densities. Yet, the theoretically restricted working voltage prevents it from progressing toward large energy densities. Efforts such as utilizing low catalytic activity electrode materials and “water-in-salt” electrolytes should be considered to broaden the voltage window even more. Moreover, the use of gel polymer electrolytes removes the requirement for a separator, which is advantageous for flexible device applications. The issue of low ionic conductivity and poor interfacial contact between the electrode material and the gel polymer electrolyte, on the other hand, should be addressed. In more cases, solid-state architecture is seen to be an efficient technique for broadening the application area of SICs devices.

#### 5. CONCLUSION

Energy usage is an essential element in human development, and the fast development of science and technology necessitates suitable energy as an assurance. The development of energy storage components has progressed and appeared as a significant key in solving the issues related to energy. The market for HICs is propelled by their distinctive electrochemical properties, which combine high  $E_d$ , quick charging time, and good cycling stability. SICs are essential because they can be utilized for extensive energy storage devices and are safer, cheaper, and more abundant on earth than LICs. In conclusion, this review examined current developments and obstacles in TMOs for encouraging their use in SICs. TMOs are one of the earliest and most promising materials that have been proposed for SICs. TMOs have significant benefits in terms of plentiful resources and inexpensive manufacturing costs. Moreover, they have a larger specific capacitance than carbon-based materials and conductive polymers. Because of their developed production technique, they have been utilized in the commercial field. Nevertheless, it has been shown that the greatest obstacle to large-scale commercial uses is their comparatively poor electrical conductivity, which limits the electrode material’s fast charge/discharge kinetics. As a result, numerous approaches have been developed to address this issue, such as the synthesis of electrode materials with nanostructures and greater active surface areas, a composite with an electrically conductive material, and multiple metal composites with synergistic effects. At the same time, the electrode material manufacturing process is growing more sophisticated. For commercial applications, the synthesis of electrode materials with high electrochemical performance via a green, ecologically friendly, easy, and low-cost technique is still required. This work reviews TMOs and sodium-based TMOs with multiple structure compounds as electrode materials for SICs in terms of specific capacitance, electrolyte type,  $E_d$ ,  $P_d$ , and capacity retention. The comparison of TMO-based electrode materials for LICs and SICs has been mentioned. This paper also highlights several significant investigations with low-cost and ecologically friendly materials such as  $\text{Na}_{0.5}\text{Mn}_{0.5}\text{Co}_{0.48}\text{Mg}_{0.02}\text{O}_2$  and  $\text{Na}_{0.44}\text{MnO}_2$ , as well as compounds with different structural types in recent studies. In recent years, the electrochemical performance of TMOs in SICs has improved steadily. The

developed SICs with high electrochemical properties that can compete with LICs will be used in battery systems in the future. SICs are expected to be crucial in both our daily lives and energy storage technologies soon.

### Acknowledgment

Miss Yamini Gupta is grateful to DST-INSPIRE for providing financial funding during the work completed.

### Conflicts of Interest

There are no conflicts of interest for the publication of this article. ♦

### REFERENCES

- ARAVINDAN, V., CHUILING, W., & MADHAVI, S. (2012). High power lithium-ion hybrid electrochemical capacitors using spinel  $\text{LiCrTiO}_4$  as insertion electrode. *Journal of Materials Chemistry*, 22(31), 16026-16031. <https://doi.org/10.1039/C2JM32970K>
- ARISTOTE, N. T., DENG, X., ZOU, K., GAO, X., MOMEN, R., & JI, X. (2022). General overview of sodium, potassium, and zinc-ion capacitors. *Journal of Alloys and Compounds*, 913, 165216. <https://doi.org/10.1016/j.jallcom.2022.165216>
- BHAT, S. S., BABU, B., FEYGENSON, M., NEUEFEIND, J. C., & SHAIJUMON, M. M. (2018). Nanostructured  $\text{Na}_2\text{Ti}_9\text{O}_{19}$  for hybrid sodium-ion capacitors with excellent rate capability. *ACS applied materials & interfaces*, 10(1), 437-447. <https://doi.org/10.1021/acsami.7b13300>
- CAI, P., ZOU, K., DENG, X., WANG, B., ZHENG, M., & JI, X. (2021). Comprehensive understanding of sodium-ion capacitors: definition, mechanisms, configurations, materials, key technologies, and future developments. *Advanced Energy Materials*, 11(16), 2003804. <https://doi.org/10.1002/aenm.202003804>
- CHEN, J., YANG, B., LIU, B., LANG, J., & YAN, X. (2019). Recent advances in anode materials for sodium-and potassium-ion hybrid capacitors. *Current Opinion in Electrochemistry*, 18, 1-8. <https://doi.org/10.1016/j.coelec.2019.07.003>
- CHEN, Z., AUGUSTYN, V., JIA, X., XIAO, Q., DUNN, B., & LU, Y. (2012). High-performance sodium-ion pseudocapacitors based on hierarchically porous nanowire composites. *ACS nano*, 6(5), 4319-4327. <https://doi.org/10.1021/nn300920e>
- CHEN, Z., YUAN, T., PU, X., YANG, H., AI, X., XIA, Y., & CAO, Y. (2018). Symmetric sodium-ion capacitor based on  $\text{Na}_{0.44}\text{MnO}_2$  nanorods for low-cost and high-performance energy storage. *ACS applied materials & interfaces*, 10(14), 11689-11698. <https://doi.org/10.1021/acsami.8b00478>
- DAS, H. T., MAIYALAGAN, T., & DAS, N. (2023). Developing potential aqueous Na-ion capacitors of  $\text{Al}_2\text{O}_3$  with carbon composites as electrode material: Recycling medical waste to sustainable energy. *Journal of Alloys and Compounds*, 931, 167501. <https://doi.org/10.1016/j.jallcom.2022.167501>
- DENG, X., ZOU, K., CAI, P., WANG, B., HOU, H., ZOU, G., & JI, X. (2020). Advanced Battery-Type Anode Materials for High-Performance Sodium-Ion Capacitors. *Small Methods*, 4(10), 2000401. <https://doi.org/10.1002/smt.202000401>
- DIEZ, N., SEVILLA, M., & FUERTES, A. B. (2023). A dual carbon Na-ion capacitor based on polypyrrole-derived carbon nanoparticles. *Carbon*, 201, 1126-1136. <https://doi.org/10.1016/j.carbon.2022.10.036>
- DING, R., QI, L., & WANG, H. (2013). An investigation of spinel  $\text{NiCo}_2\text{O}_4$  as anode for Na-ion capacitors. *Electrochimica Acta*, 114, 726-735. <https://doi.org/10.1016/j.electacta.2013.10.113>
- DONG, S., LV, N., WU, Y., ZHU, G., & DONG, X. (2021). Lithium-ion and sodium-ion hybrid capacitors: from insertion-type materials design to devices construction. *Advanced Functional Materials*, 31(21), 2100455. <https://doi.org/10.1002/adfm.202100455>
- DONG, S., SHEN, L., LI, H., NIE, P., ZHU, Y., SHENG, Q., & ZHANG, X. (2015). Pseudocapacitive behaviors of  $\text{Na}_2\text{Ti}_3\text{O}_7$ @CNT coaxial nanocables for high-performance sodium-ion capacitors. *Journal of Materials Chemistry A*, 3(42), 21277-21283. <https://doi.org/10.1039/C5TA05714K>
- DONG, S., SHEN, L., LI, H., PANG, G., DOU, H., & ZHANG, X. (2016). Flexible sodium-ion pseudocapacitors based on 3D  $\text{Na}_2\text{Ti}_3\text{O}_7$  nanosheet arrays/carbon textiles anodes. *Advanced Functional Materials*, 26(21), 3703-3710. <https://doi.org/10.1002/adfm.201600264>
- FAN, Y., LI, C., LIU, X., REN, J., ZHANG, Y., CHI, J., & WANG, L. (2023). Honeycomb structured nano MOF for high-performance sodium-ion hybrid capacitor. *Chemical Engineering*



- Journal, 452, 139585. <https://doi.org/10.1016/j.cej.2022.139585>
- FANG, Y., ZHANG, Y., MIAO, C., ZHU, K., CHEN, Y., & CAO, D. (2020). MXene-derived defect-rich  $\text{TiO}_2/\text{TGO}$  as high-rate anodes for full Na ion batteries and capacitors. *Nano-micro letters*, 12(1), 1-16. <https://doi.org/10.1007/s40820-020-00471-9>
- GAO, L., CHEN, G., ZHANG, L., YAN, B., & YANG, X. (2021). Engineering pseudocapacitive  $\text{MnMoO}_4/\text{C}$  microrods for high energy sodium ion hybrid capacitors. *Electrochimica Acta*, 379, 138185. <https://doi.org/10.1016/j.electacta.2021.138185>
- GAO, L., CHEN, S., ZHANG, L., & YANG, X. (2018). High performance sodium ion hybrid supercapacitors based on  $\text{Na}_2\text{Ti}_3\text{O}_7$  nanosheet arrays. *Journal of Alloys and Compounds*, 766, 284-290. <https://doi.org/10.1016/j.jallcom.2018.06.288>
- GAO, L., HUANG, D., SHEN, Y., & WANG, M. (2015). Rutile- $\text{TiO}_2$  decorated  $\text{Li}_4\text{Ti}_5\text{O}_{12}$  nanosheet arrays with 3D interconnected architecture as anodes for high performance hybrid supercapacitors. *Journal of Materials Chemistry A*, 3(46), 23570-23576. <https://doi.org/10.1039/C5TA07666H>
- GU, H., KONG, L., CUI, H., ZHOU, X., XIE, Z., & ZHOU, Z. (2019). Fabricating high-performance sodium ion capacitors with  $\text{P2-Na}_{0.67}\text{Co}_{0.5}\text{Mn}_{0.5}\text{O}_2$  and MOF-derived carbon. *Journal of Energy Chemistry*, 28, 79-84. <https://doi.org/10.1016/j.jechem.2018.01.012>
- GUI, Q., BA, D., ZHAO, Z., MAO, Y., ZHU, W., & LIU, J. (2019). Synergistic Coupling of Ether Electrolyte and 3D Electrode Enables Titanates with Extraordinary Coulombic Efficiency and Rate Performance for Sodium-Ion Capacitors. *Small Methods*, 3(2), 1800371. <https://doi.org/10.1002/smt.201800371>
- HALDER, B., RAGUL, S., SANDHIYA, S., & ELUMALAI, P. (2023). Flexible Solid-State Aqueous Sodium-Ion Capacitor Using Mesoporous Self-Heteroatom-Doped Carbon Electrodes. *ACS Applied Electronic Materials*. <https://doi.org/10.1021/acsaelm.2c01474>
- HAN, C., WANG, X., PENG, J., XIA, Q., CHOU, S., & LI, W. (2021). Recent progress on two-dimensional carbon materials for emerging post-lithium ( $\text{Na}^+$ ,  $\text{K}^+$ ,  $\text{Zn}_2^+$ ) hybrid supercapacitors. *Polymers*, 13(13), 2137. <https://doi.org/10.3390/polym13132137>
- HENGHENG, X. I. A., ZHONGXUN, A. N., TINGLI, H. U. A. N. G., WENYING, F. A. N. G., LIANHUAN, D. U., & LI, H. U. A. (2018). Construction of Li-ion supercapacitor-type battery using active carbon/ $\text{LiNi}_{0.5}\text{Co}_{0.2}\text{Mn}_{0.3}\text{O}_2$  composite as cathode and its electrochemical performances. *Energy Storage Science and Technology*, 7(6), 1233. <https://doi.org/10.12028/j.issn.2095-4239.2018.0142>
- JIA, R., SHEN, G., & CHEN, D. (2020). Recent progress and future prospects of sodium-ion capacitors. *Science China Materials*, 63(2), 185-206. <https://doi.org/10.1007/s40843-019-1188-x>
- JIANG, Y., TAN, S., WEI, Q., DONG, J., LI, Q., XIONG, F., ... & MAI, L. (2018). Pseudocapacitive layered birnessite sodium manganese dioxide for high-rate non-aqueous sodium ion capacitors. *Journal of Materials Chemistry A*, 6(26), 12259-12266. <https://doi.org/10.1039/C8TA02516A>
- JO, A., LEE, B., KIM, B. G., LIM, H., HAN, J. T., & PARK, J. H. (2023). Ultrafast laser micromachining of hard carbon/fumed silica anodes for high-performance sodium-ion capacitors. *Carbon*, 201, 549-560. <https://doi.org/10.1016/j.carbon.2022.09.031>
- KARIKALAN, N., KARUPPIAH, C., CHEN, S. M., VELMURUGAN, M., & GNANAPRAKASAM, P. (2017). Three-dimensional fibrous network of  $\text{Na}_{0.21}\text{MnO}_2$  for aqueous sodium-ion hybrid supercapacitors. *Chemistry-A European Journal*, 23(10), 2379-2386. <https://doi.org/10.1002/chem.201604878>
- KIM, H. J., RAMASAMY, H. V., JEONG, G. H., ARAVINDAN, V., & LEE, Y. S. (2020). Deciphering the Structure-Property Relationship of Na-Mn-Co-Mg-O as a Novel High-Capacity Layered-Tunnel Hybrid Cathode and Its Application in Sodium-Ion Capacitors. *ACS applied materials & interfaces*, 12(9), 10268-10279. <https://doi.org/10.1021/acsaami.9b19288>
- LE, Z., LIU, F., NIE, P., LI, X., LIU, X., & LU, Y. (2017). Pseudocapacitive sodium storage in mesoporous single-crystal-like  $\text{TiO}_2$ -graphene nanocomposite enables high-performance sodium-ion capacitors. *ACS nano*, 11(3), 2952-2960. <https://doi.org/10.1021/acsnano.6b08332>
- LEE, S. Y., AN, J. H., & PARK, Y. I. (2023). Synergistic effect of  $\text{NaTi}_2(\text{PO}_4)_3$  and MXene synthesized in situ for high-performance sodium-ion capacitors. *Applied Surface Science*, 612, 155960. <https://doi.org/10.1016/j.apsusc.2022.155960>
- LENG, K., ZHANG, F., ZHANG, L., ZHANG, T., WU, Y., & CHEN, Y. (2013). Graphene-based Li-ion hybrid supercapacitors with ultrahigh performance. *Nano Research*, 6, 581-592. <https://doi.org/10.1007/s12274-013-0334-6>

- LI, T., GAO, Q., LIU, S., ZHANG, X., ZHANG, Y., & YUAN, C. (2023). Facile Construction of Nano-Dimensional Bi Encapsulated in N-Doped Porous Carbon Frameworks for High-Performance Sodium-Ion Hybrid Capacitors. *ACS Applied Energy Materials*. <https://doi.org/10.1021/acsaem.3c00003>
- LIANG, H., ZHANG, H., ZHAO, L., CHEN, Z., HUANG, C., & LI, H. (2022). Layered  $\text{Fe}_2(\text{MoO}_4)_3$  assemblies with pseudocapacitive properties as advanced materials for high-performance sodium-ion capacitors. *Chemical Engineering Journal*, 427, 131481. <https://doi.org/10.1016/j.cej.2021.131481>
- LIM, E., JO, C., KIM, M. S., KIM, M. H., CHUN, J., & LEE, J. (2016). High-performance sodium-ion hybrid supercapacitor based on  $\text{Nb}_2\text{O}_5$ @ carbon core-shell nanoparticles and reduced graphene oxide nanocomposites. *Advanced Functional Materials*, 26(21), 3711-3719. <https://doi.org/10.1002/adfm.201505548>
- LIU, L., DU, Z., SUN, J., HE, S., WANG, K., & AI, W. (2023). Engineering the First Coordination Shell of Single Zn Atoms via Molecular Design Strategy toward High-Performance Sodium-Ion Hybrid Capacitors. *Small*, 2300556. <https://doi.org/10.1002/sml.202300556>
- LIU, L., ZHAO, Z., HU, Z., LU, X., ZHANG, S., & LI, H. (2020). Designing Uniformly Layered  $\text{FeTiO}_3$  Assemblies Consisting of Fine Nanoparticles Enabling High-Performance Quasi-Solid-State Sodium-Ion Capacitors. *Frontiers in Chemistry*, 8, 371. <https://doi.org/10.3389/fchem.2020.00371>
- LIU, Z., ZHANG, X., HUANG, D., GAO, B., NI, C., & WANG, G. (2020). Confined seeds derived sodium titanate/graphene composite with synergistic storage ability toward high performance sodium ion capacitors. *Chemical Engineering Journal*, 379, 122418. <https://doi.org/10.1016/j.cej.2019.122418>
- MAURYA, D. K., MURUGADOSS, V., GUO, Z., & ANGAIAH, S. (2021). Designing  $\text{Na}_2\text{Zn}_2\text{TeO}_6$ -Embedded 3D-Nanofibrous Poly (vinylidene-fluoride)-co-hexafluoropropylene-Based Nanohybrid Electrolyte via Electrospinning for Durable Sodium-Ion Capacitors. *ACS Applied Energy Materials*, 4(8), 8475-8487. <https://doi.org/10.1021/acsaem.1c01682>
- PENG, H., HAN, S., ZHAO, J., KLIMOVA-KORSMIK, O., TOLOCHKO, O. V., & WANG, G. K. (2023). 2D Heterolayer-Structured  $\text{MoSe}_2$ -Carbon with Fast Kinetics for Sodium-Ion Capacitors. *Inorganic Chemistry*. <https://doi.org/10.1021/acs.inorgchem.2c03819>
- QIN, J., SARI, H. M. K., WANG, X., YANG, H., ZHANG, J., & LI, X. (2020). Controlled design of metal oxide-based ( $\text{Mn}^{2+}/\text{Nb}^{5+}$ ) anodes for superior sodium-ion hybrid supercapacitors: Synergistic mechanisms of hybrid ion storage. *Nano Energy*, 71, 104594. <https://doi.org/10.1016/j.nanoen.2020.104594>
- QUE, L. F., YU, F. D., HE, K. W., WANG, Z. B., & GU, D. M. (2017). Robust and conductive  $\text{Na}_2\text{Ti}_2\text{O}_5$ -x nanowire arrays for high-performance flexible sodium-ion capacitor. *Chemistry of Materials*, 29(21), 9133-9141. <https://doi.org/10.1021/acs.chemmater.7b02864>
- SONG, Y., PENG, Y., LI, H., SUN, X., LI, L., ZHANG, C., & YIN, F. (2022).  $\text{Mn}_3\text{O}_4$  Nanoparticles In Situ Embedded in  $\text{TiO}_2$  for High-Performance Na-ion capacitor: Balance between 3D Ordered Hierarchically Porous Structure and Heterostructured Interfaces. *Chemical Engineering Journal*, 137450. <https://doi.org/10.1016/j.cej.2022.137450>
- SU, H., JAFFER, S., & YU, H. (2016). Transition metal oxides for sodium-ion batteries. *Energy storage materials*, 5, 116-131. <https://doi.org/10.1016/j.ensm.2016.06.005>
- SUN, C., ZHANG, X., AN, Y., LI, C., WANG, L., & MA, Y. Low-temperature carbonized nitrogen-doped hard carbon nanofiber towards high-performance sodium-ion capacitors. *Energy & Environmental Materials*, e12603. <https://doi.org/10.1002/eem2.12603>
- THIRUMAL, V., SREEKANTH, T. V. M., YOO, K., & KIM, J. (2023). Biomass-Derived Hard Carbon and Nitrogen-Sulfur Co-Doped Graphene for High-Performance Symmetric Sodium Ion Capacitor Devices. *Energies*, 16(2), 802. <https://doi.org/10.3390/en16020802>
- TIAN, S., QI, L., & WANG, H. (2016). A  $\text{Na}^+$ -storage electrode material free of potential plateaus and its application in electrochemical capacitors. *Solid State Ionics*, 289, 194-198. <https://doi.org/10.1016/j.ssi.2016.03.010>
- WANG, G., OSWALD, S., LÖFFLER, M., MÜLLEN, K., & FENG, X. (2019). Beyond Activated Carbon: Graphite-Cathode-Derived Li-Ion Pseudocapacitors with High Energy and High Power Densities. *Advanced Materials*, 31(14), 1807712. <https://doi.org/10.1002/adma.201807712>
- WANG, M., PENG, A., JIANG, J., ZENG, M., YANG, Z., & LI, X. (2022). Heterointerface synergistic

- Na<sup>+</sup> storage fundamental mechanism for CoSeO<sub>3</sub> playing as anode for sodium ion batteries/capacitors. *Chemical Engineering Journal*, 433, 134567. <https://doi.org/10.1016/j.cej.2022.134567>
- WANG, S., ZHAO, H., LV, S., JIANG, H., SHAO, Y., & LEI, Y. (2021). Insight into Nickel-Cobalt Oxy-sulfide Nanowires as Advanced Anode for Sodium-Ion Capacitors. *Advanced Energy Materials*, 11(18), 2100408. <https://doi.org/10.1002/aenm.202100408>
- XIANG, J., ZHANG, P., LV, S., MA, Y., ZHAO, Q., & QIN, C. (2021). Spinel LiMn<sub>2</sub>O<sub>4</sub> nanoparticles fabricated by the flexible soft template/Pichini method as cathode materials for aqueous lithium-ion capacitors with high energy and power density. *RSC advances*, 11(25), 14891-14898. <https://doi.org/10.1039/D0RA07823A>
- YANG, C., LAN, J. L., LIU, W. X., LIU, Y., YU, Y. H., & YANG, X. P. (2017). High-performance Li-ion capacitor based on an activated carbon cathode and well-dispersed ultrafine TiO<sub>2</sub> nanoparticles embedded in mesoporous carbon nanofibers anode. *ACS Applied Materials & Interfaces*, 9(22), 18710-18719. <https://doi.org/10.1021/acsami.7b02068>
- YANG, D., ZHAO, Q., HUANG, L., XU, B., KUMAR, N. A., & ZHAO, X. S. (2018). Encapsulation of NiCo<sub>2</sub>O<sub>4</sub> in nitrogen-doped reduced graphene oxide for sodium ion capacitors. *Journal of Materials Chemistry A*, 6(29), 14146-14154. <https://doi.org/10.1039/C8TA03411G>
- YANG, S., JIANG, J., HE, W., WU, L., XU, Y., & ZHANG, X. (2023). Nitrogen-doped carbon encapsulating Fe<sub>7</sub>Se<sub>8</sub> anode with core-shell structure enables high-performance sodium-ion capacitors. *Journal of Colloid and Interface Science*, 630, 144-154. <https://doi.org/10.1016/j.jcis.2022.10.034>
- YUAN, C., WU, H. B., XIE, Y., & LOU, X. W. (2014). Mixed transition-metal oxides: design, synthesis, and energy-related applications. *Angewandte Chemie International Edition*, 53(6), 1488-1504. <https://doi.org/10.1002/anie.201303971>
- ZHANG, H., HU, M., LV, Q., HUANG, Z. H., KANG, F., & LV, R. (2020). Advanced Materials for Sodium-Ion Capacitors with Superior Energy-Power Properties: Progress and Perspectives. *Small*, 16(15), 1902843. <https://doi.org/10.1002/sml.201902843>
- ZHANG, H., LIU, B., LU, Z., HU, J., XIE, J., HAO, A., & CAO, Y. (2023). Sulfur-Bridged Bonds Heightened Na-Storage Properties in MnS Nanocubes Encapsulated by S-Doped Carbon Matrix Synthesized via Solvent-Free Tactics for High-Performance Hybrid Sodium-Ion Capacitors. *Small*, 2207214. <https://doi.org/10.1002/sml.202207214>
- ZHANG, T., WANG, R., HE, B., JIN, J., GONG, Y., & WANG, H. (2021). Recent advances on pre-sodiation in sodium-ion capacitors: A mini review. *Electrochemistry Communications*, 129, 107090. <https://doi.org/10.1016/j.elecom.2021.107090>
- ZHANG, X., CHEN, S., CAI, J., KING, S., LIU, C., & WANG, G. (2023). Pre-strain accommodation enabled multi-dimensionally and hierarchically elastomeric MoSe<sub>2</sub>/MXene and AC/MXene electrodes for stretchable sodium-ion capacitors. *Journal of Alloys and Compounds*, 935, 168065. <https://doi.org/10.1016/j.jallcom.2022.168065>
- ZHANG, Y., AN, Y., JIANG, J., DONG, S., WU, L., & ZHANG, X. (2018). High Performance Aqueous Sodium-Ion Capacitors Enabled by Pseudocapacitance of Layered MnO<sub>2</sub>. *Energy Technology*, 6(11), 2146-2153. <https://doi.org/10.1002/ente.201800157>
- ZHANG, Y., JIANG, J., AN, Y., WU, L., DOU, H., & GUO, Z. (2020). Sodium-ion capacitors: materials, mechanism, and challenges. *ChemSusChem*, 13(10), 2522-2539. <https://doi.org/10.1002/cssc.201903440>
- ZHOU, J., YANG, K., KANG, Q., LIU, C., LI, X., & HOU, W. (2023). Fast electrochemical redox kinetics of two-dimensional TiO<sub>2</sub>/Ti<sub>3</sub>C<sub>2</sub>T<sub>x</sub> (MXene) heterostructure for high-performance lithium-ion capacitor. *Journal of Electroanalytical Chemistry*, 928, 117034. <https://doi.org/10.1016/j.jelechem.2022.117034>
- ZHU, J., ROSCOW, J., CHANDRASEKARAN, S., DENG, L., ZHANG, P., & HUANG, L. (2020). Biomass-derived carbons for sodium-ion batteries and sodium-ion capacitors. *ChemSusChem*, 13(6), 1275-1295. <https://doi.org/10.1002/cssc.201902685>
- ZHU, Y. E., YANG, L., SHENG, J., CHEN, Y., GU, H., WEI, J., & ZHOU, Z. (2017). Fast sodium storage in TiO<sub>2</sub>@CNT@C nanorods for high-performance Na-ion capacitors. *Advanced Energy Materials*, 7(22), 1701222. <https://doi.org/10.1002/aenm.201701222>





**Publisher's note:** Eurasia Academic Publishing Group (EAPG) remains neutral with regard to jurisdictional claims in published maps and institutional affiliations.

**Open Access.** This article is licensed under a Creative Commons Attribution-NoDerivatives 4.0 International (CC BY-ND 4.0) licence, which permits copy and redistribute the material in any medium or format for any purpose, even commercially. The licensor cannot revoke these freedoms as long as you follow the licence terms. Under the following terms you must give appropriate credit, provide a link to the license, and indicate if changes were made. You may do so in any reasonable manner, but not in any way that suggests the licensor endorsed you or your use. If you remix, transform, or build upon the material, you may not distribute the modified material. To view a copy of this license, visit <https://creativecommons.org/licenses/by-nd/4.0/>.